NIPES

Journal of Energy Technology and Environment

Journal homepage: www.nipesjournals.org.ng

Engine Performance Evaluation of Biodiesel Produced from Watermelon using Modified Catalyst.

Ekere, P. O., [1*], Obanor, A. I., [2], Amenaghawon, A., N., [3]

[1]Projects Development Institute (PRODA), Emene, Enugu, Enugu State, Nigeria.
[2]Mechanical Engineering Department, University of Benin, Benin City, Edo State, Nigeria.
[3]Chemical engineering Department, University of Benin, Benin City, Edo State, Nigeria.
*Corresponding Author: ekerepius973@gmail.com (+2348033605605)

Article information

Article History
Received 14 March 2024
Revised 9 April 2024
Accepted 9 May 2024
Available online 1 June 2024

Keywords:
Chain Management, Challenges, Strategies, Sustainability, Communication

https://doi.org/10.5281/zenodo.11408439

https://nipes.org

Abstract

This study used a composite catalyst consisting of marble and periwinkle doped with barium to produce biodiesel from watermelon and its performance and emission characteristics was evaluated with a diesel engine. The physiochemical features of the oil and fatty acid methyl ester were determined using acceptable protocols outlined in (ASTM) 6751(1973) to investigate the impact of the triglyceride's properties and the biodiesel was produced by transesterification reaction. The engine performance and emission characteristics of the biodiesel was carried out using Perkins 4:108 diesel engine test bed. The properties of the watermelon seed oil showed that they do not require pre-treatment before transesterification and the yield under the process parameters; catalyst weight of 6.83 wt%, methanol/oil molar ratio 9.69:1, temperature of 61℃, time of 3.48 hours and speed of 295 rpm was 87.64 %. The engine performance revealed that the biodiesel blends exhibited higher brake power than conventional diesel but B20 has similar thermal efficiency with B0. Additionally, the blends of biodiesel showed reduced emissions as compared to regular fuel. With very little gaseous pollution emissions, the engine evaluation metrics of the biodiesel mix, particularly B20, were comparable to those of conventional diesel fuel.

1. Introduction

The most affordable internal combustion engine type for use in power-generating engineering machinery is the diesel engine[1,2]. These engines play a significant role in transportation (road, railway, naval) and electricity generation, contributing significantly to global economic activity. Fossil fuels are the primary source of fuel for diesel engines due to their high thermal efficiency, which results in excellent engine performance. However, the combustion of these fuels produces pollutants such as CO2, CO, NOx, and PM, which pose a threat to the environment through air pollution and global warming[3]. The high energy demand and limited petroleum reserves lead to a rapid depletion of fossil fuels with an estimated 40-year lifespan[2]. These elements have spurred development of alternative diesel fuels with an emphasis on environmental pollution minimization and maximum efficiency [4].

One of the renewable fuels that have attracted attention worldwide is biodiesel. Finding new and renewable energy sources other than hydro, biomass, wind, solar, geothermal, hydrogen, and nuclear power is therefore crucial [5]. Free fatty acid methyl esters (FAME), commonly known as biodiesel comes from sources of fat and oil. For diesel-powered vehicles, it is a clean-burning, sustainable, renewable, and nontoxic fuel that burns cleanly [3, 6, 7]. Vegetable oils present certain issues due to their low volatility, substantial viscosity, and polyunsaturated nature, rendering them unsuitable for use in diesel-powered vehicles. In order to synthesize biodiesel from plant-based oil and/or animal fats for unmodified consumption as a fuel substitute in diesel-powered vehicles, some methods for overcoming these challenges include the immediate application or mixing of oils, micro-emulsification with alcohols, visbreaking or devolatilization, and alcoholysis [6, 8, 9]. The most critical step in producing cleaner, biodegradable fuel is alcoholysis (transesterification). It also saves money and time and produces fuel that executes better and has a greater cetane number [10, 11].

Engine evaluation is necessary to ascertain whether biodiesel is appropriate for usage in diesel engines [12].According to Dandajeh et al. [13], adding a small amount water up to 4 weight percent to diesel and rapeseed methyl ester substantially lowered exhaust gases, especially for NOx, CO, and CO_2. They looked into the combustion emission parameters of a gardener compressed-ignition engine fuelled with rapeseed methyl and fossil diesel. According to reports, biodiesel dramatically decreased emissions of PM, HC, CO, and CO_2, but also produced somewhat greater emissions of NOx. Research further demonstrated that NOx emissions might be decreased by mixing with stabilizers [14]. Literatures also shown that the 20% biodiesel blend with diesel lowers smoke, CO and hydrocarbon emissions [15, 16]. The most widely acknowledged explanation for the rise in NOx, according to Adaileh et al. [17], is that the biodiesel's higher cetane number shortens the ignition delay, which in turn increases NOx emissions because it lengthens the burning mixture's duration in the cylinder. Because neat biodiesel has 11% oxygen by weight, it burns more fully and emits fewer emissions from unburned fuel. The Environmental Protection Agency (EPA) concludes that biodiesel has positive and predictable benefits to the environment. Bjorn and Capareda[18] found similar results, supporting the usage of biodiesel as a diesel engine fuel substitute due to its ability to run in any compression ignition engine with little to no modification. Ude, et al. [3] looked at the appraisement of cottonseed oil biodiesel manufactured using calcium oxide and prediction using a machine learning network, they discovered comparable results. Som et al. [19] demonstrated that due to reduced vapour pressure of biodiesel, it was found to have a lower cavitation rate than petro-diesel. Pereira et al. [20] claim that because biodiesel has a higher flash point and superior lubricity compared to diesel fuel, its manipulation is safer and results in fewer scratches on the fuel injecting mechanism's components.

Moreso, Gulzal et al. [21] investigated the long-term compatibility of biodiesel in a modern diesel engine family, concentrating on its interactions with engine lubricant. They subjected the compression ignition (CI) engines powered with diesel or a biodiesel-diethyl ester B20 combination to a long-run endurance test. When compared to the diesel, the outcome indicated a minor increase in wear and friction. According to Fashe et al. [22], excellent lubrication is a critical component of biodiesel since it minimizes wear and friction on sliding parts and increases engine longevity when set side by side to conventional diesel. Fatzal et al. [23] and Fathurrahman et al. [24] examined the frictional parameters of vegetable oil biodiesel and its blends under continuous load at various agitation speeds ranging from 600 to 1500 rpm. The findings demonstrated that frictional effect reduced as the amount of biodiesel rose, and that adding biodiesel effectively reduced attrition on the sliding parts. The majority of the researchers demonstrated that while utilizing biodiesel from different raw materials in diesel engines increased brake specific fuel consumption (BSFC) compared to diesel engines, it only slightly decreased brake power (Bp) and brake thermal efficiency

(BTE)[2, 3, 11, 25]. For instance, China and India government utilized 15 percent biodiesel blended with petrol-diesel in 2020, while the Malaysian government lunched B10 in 2019, which was raised to B20 in 2020 [26, 27].

African countries like Nigeria, Ghana etchave keyed in to this new trend on biofuels but are yet to start its application despite being endowered with raw material for their production.Aboje et al. [28] studied the optimization and characterization of biodiesel production from Desert Date seed oil (*Balanites aegyptiaca*) and obtained 92% yield. Ude et al. [11] evaluated engine performance and emission of African pear seed oil (APO) biodiesel and its prediction via multi-input-multi-output artificial neural network (ANN) and sensitivity analysis. They discovered that blending 20% of biodiesel with diesel performed optimally in I.C. engine without modification. Their results are in consistent with those of Elendu et al. [2] who studied the yield optimization and fuel properties evaluation of the biodiesel derived from avocado pear waste. The limited application of biodiesel in Nigeria could be due to few research on its engine performance. Therefore, this study focused on engine performance evaluation of biodiesel and its blends from watermelon seed oil.

2. Material and Methods

2.1 Materials

Watermelon (Citrullus lanatus) seeds oil was bought from Danchadi Market in Bodinga L.G.A, Sokoto State, Nigeria. The petro-diesel was purchased from North West Filling Station, Emene, Enugu, Enugu State, Nigeria. All the reagentsutilized such as aqueous potassium hydroxide, ethanol, chloroform, potassium iodide, sodium thiosulphate, sodium hydroxide and methanol, were of standard for analysis, and acquired from De Integrated Chemicals Ltd, Ogbete Enugu State, Nigeria and used as such without further treatment.

2.2 Methods

2.2.1 Oil Characterization

The extraction of oil from watermelon seeds was carried out using a solvent extraction technique with n-hexane as the solvent and adopted the method employed by Ude et al. [11]. The oil extracted was analyzed to determine their properties and free fatty acid (FFA) composition. The physiochemical properties that were determined are; viscosity, specific gravity, calorific value, Cetane number, pour point, FFA, cloud point, flash point, iodine value and saponification value. All of these characteristics were ascertained using the American Society for Testing Material's ASTM 6751 [29] and ASTM D4067 [30] guidelines, as well as equipment like Fourier transform infrared spectrometers and gas chromatography mass spectrometers for fatty acids and structural group.

2.2.2 Catalyst Preparation and characterization

The modified marble-periwinkle composite CaO used in this work is a heterogeneous catalyst that was created using the same process as Manuit and Statit[31]. Two hundred and fifty grammes (250g) each of grounded marble chips and periwinkle was mixed and immersed in 500 mL of distilled water in a 1000 L volumetric flask. Fifty grammes (50g) of barium sulphate was added to the mixture and manually stirred vigorously to obtain a homogeneous mixture. The mixture was kept in a water bath (DK-420, Techmel & Techmel, USA) for 2h at temperature of 70^{o}C. It was then filtered to remove water and the residue (marble-periwinkle composite) was dried in an oven at a temperature of 110^{o}C for 4h. The dried composite was heat treated in an inert muffle furnace for four hours at 800 degrees Celsius to thermally activate it.

Then, the ASTM D4067 [30] method was utilized to describe the physiochemical parameters of both raw and activated CaO samples. X-ray Diffractometer, scanning electron microscope, Fourier transform infra-red spectrometer and X-ray fluorescent were used to ascertain the mineralogy/type, the morphology, functional group and metallic compositions of the catalyst.

2.2.3 Biodiesel synthesis and characterization

The extracted oils from watermelon seed reacted with methanol in the presence of thermally activated CaO to produce methyl esters of fatty acids (biodiesel) and glycerol. Fifty gram of the oil was poured into a flat bottom flask mounted on a heating magnetic stirrer. Twenty-four millilitres (24 mL representing 9.69:1 molar ratio) of methanol was then added together with a 3.415 g amount of catalyst (6.83 wt% of the oil). Throughout the reaction, the reaction flask was maintained at a consistent temperature of 61^{o}C and with 295 rpm agitation on a hot magnetic stirrer. After 1 h the sample was removed, allowed to cool, and the biodiesel (by settling overnight under ambient conditions, the by-product (i.e., the glycerol in the lower layer) was separated from the methyl ester in the upper layer. By weighing the layer biodiesel and the amount of oil utilized, the percentage of the biodiesel production was calculated.

$$Y = \frac{weight\ of\ biodiesel}{weight\ of\ oil\ used}\ x\ 100 \quad (1)$$

The biodiesel was characterized using ASTM to determine its physical and chemical properties.

2.2.4 Engine Performance

The performance of the biodiesel produced by the transesterification process was evaluated on a PERKINS 4:108 SINGLE CYLINDER DIESEL ENGINES mounted on a steady state engine test bed developing a power output of 1212 kW at 3000 rpm. It has a bore of 79.735 mm, a stroke of 88.9 mm, a swept volume of 1.76 L/cycle, and a compression ratio of 18. An electrical dynamometer is used for loading the engine. It has an orifice that measures the flow of air from the Perkins engine. This engine is a 4-stroke, naturally aspirated, water-cooled compression ignition (CI) engine with four cylinders. The engine's specifications are listed in Table 1, and Figure1 display the experimental setup. Standard diesel fuel, mixes, and biodiesel were used in the studies.

Test was performed indoors at ambient temperature of 30 °C and 29% of humidity. Before the test, a brief trial run was conducted to make sure that all necessary accessories were in operational order. Engine performance trials were conducted at various engine speeds between 1400 and 2000 rpm while maintaining a constant 100 kg load. High blends of biodiesel-diesel (B20, B60, B100, and B0) were utilized in the experiment since the viscosities of the methyl esters generated from watermelon seed oil were within the ASTM permissible limit for biodiesel. As a precaution, the engine was warmed up using just pure diesel until the cooling water temperature hit 80 degrees Celsius. The previously indicated loads and speeds were applied to the engine. The amount of time it took to use a certain volume (50 ml) of fuel at each speed was timed using a stop watch. Measurements were made of the torque, exhaust temperature, and manometer reading. Next, calculations were made for the braking power, brake specific fuel consumption (BSFC), and brake thermal efficiency.

In addition, different weights (50, 100, 150, and 200 kg) were added to the engine and it was reloaded at a constant 2000 rpm. The engine's load was adjusted using the dynamometer loading wheel. Using a portable digital gas analyzer, the exhaust gases, including carbon (IV) oxide, (CO) and hydrocarbon (HC), were analysed (BACHARACH B). The engine's exhaust pipe end was used to collect the emission data. Utilizing the measured densities of diesel and biodiesel through

Equations (2) and (3), the fuel consumption is evaluated by measuring the fuel consumed per unit time and the computed values of each blend's density according to Ude et al. [3].

$$3.\dot{m}_f = \rho_b Q_f \quad (2)$$

$$4.\rho_b = \sum \rho_i v_i \quad (3)$$

Where $\dot{m}_f$= diesel mass flow rate, (kg/s), ρ_b= odiesel density, (kg/m^3), Q_f= biodiesel volumetric flow rate, (m^3/s), ρ_i = density of biodiesel or diesel, (kg/m^3), v_i= composition of biodiesel or diesel, (%).

Table 1: Specifications of the Diesel Engine Test Bed (1212Kw)

Components	Values
Type	Perkins 4:108
Bore	79.74mm
Stroke	89mm
SV	1.8 L/cycle
CR	22:1
Max. BHP	38 hp
Max. speed	3000 rpm
NCH	4
DoE	$1\frac{1}{2}''$
LEP	$36\ 31'$
Dynamometer capacity	112 kW/150 hp
Dynamometer Max. Speed	7500 rpm
Power	(N_mx rev/min)/9549.31 (kW)
Fuel guage	50-100cc

SV=swept volume, CR = compression ratio, number of cylinder head, diameter of exhaust, length of exhaust.

Figure 1: Diesel Engine Test Bed.

The fuel's cetane number was evaluated using the sample's aniline point (AP) and degree API at specific gravity. An aniline solution was introduced to the biodiesel in a flask in order to measure

the biodiesel's aniline point. The blend was agitated and heated on an electric heater until they combined to form a homogenous solution. The beaker and its contents were allowed to cool before the heating was turned off and a thermometer was placed inside. The aniline point is the temperature at which the two phases split and was measured. The following formula were used to calculate the sample's degree API and Diesel index.

$$Degree\ API = \frac{141.5}{Specific\ gravity\ at\ 60℃} - 131.5 \quad (4)$$

$$Diesel\ index\ (DI) = \frac{Degree\ API * Aniline\ point}{100} \quad (5)$$

Lastly, the following formula was used to find the sample's cetane number[3]:

$$Cetane\ Number = 0.72\ DI + 10 \quad (6)$$

3. Result and Discussion

3.1 Physical and chemical characteristics of the oil

Table 2 presents the physical and chemical features of the raw oil of watermelon. The oil has a relatively small free fatty acid value of 0.558% and an average acid number of 1.115 mgKOH/g. According to these amounts, homogeneous and heterogeneous catalysts can both be used to trans-esterify the oil without requiring any prior pretreatment. Because of its high viscosity and density, the oil cannot be used directly as biofuel in internal combustion engines due to difficulties in the atomization process. The oil's low pour point, a sign that it won't solidify much at room temperature, allows it to be kept for an extended amount of time. The oil can be used to make biodiesel because of its strong oxidation stability. The exceptional oxidation stability of the oils could potentially be attributed to the extraction method utilized. Upon solvent extraction, base oil is recovered together with a small amount of naturally occurring antioxidant sulfur compounds.

Table 2: Physical and chemical characteristics of watermelon seed oil, WMSO

S/N	Properties	Watermelon seed oil
1	Sp. gr.	0.983
2	AV (mgKOHg)	1.115
3	FFA (%)	0.558
4	SV (mgKOH/g)	191
5	IV (gI_2/100g)	5.99
6	KV at 40^{o}C (mm^2/s)	58.31
7	PV	1.27
8	FP	78
9	CP	-3
10	PP	13
11	MC (%)	0.08
12	RI	1.47
13	Oxidation stability 11^{o}C (Hour)	5
14	MW	868.3

Sp. gr= specific gravity, AV = acid value, FFA= free fatty acid, SV= saponification value, IV= iodine value, KV = kinematics viscosity, PV = peroxide value, FP = flash point, CP=cloud point,PP=pour point, MC=moisture content, RI=refractive index, MW= molecular weight.

The fatty acid composition/profile of watermelon seed oil was carried out with the aid of Gas Chromatography Mass Spectrometry (GC-MS). The fatty acid composition of watermelon seed is shown in Table 3. According to the table, watermelon oil is made up of 89.97% unsaturated acids (oleic, linoleic, and linolenic) and 10.03% saturated acids (lauric, myristic, palmitic, and arachidic acids). The oil falls into the linoleic acid category because linolenic acid, which made up 81.29% of the total fatty acid composition, was the predominant tri-unsaturated fatty acid. This is consistent with Ogunsuyi's[32]claim of 76% oleic acid concentration. This demonstrates that the triglycerides in watermelon seed oil are extremely unsaturated. However, it was discovered that the fatty acid composition of the watermelon seed oil matched that of the common oils used to make biodiesel.

Table 3: Fatty acid composition of watermelon seed oil.

S/N	FFA Profile		Watermelon seed oil
	Fatty Acid	Component	Composition (%)
1	Capric	C_{10}	1.04
2	Lauric	C_{12}	1.33
3	Myristic	C_{14}	0.65
4	Palmitic	$C_{16:0}$	0.31
5	Magaric	C_{17}	3.40
6	Stearic	$C_{18:0}$	1.08
7	Oleic	$C_{18:1}$	4.42
8	Linoleic	$C_{18:2}$	4.26
9	Linolenic	$C_{18:3}$	81.29
10	Arachidic	C_{20}	2.22
11	Euric	C_{21}	-
	Total		100

Figure 2 displays the watermelon seed oil's Fourier transform infra-red (FTIR) spectrum. To determine which functional groups were present in the feedstock, this was done. The result shows some quite noticeable peaks. The range 723.1 - 913.2 cm^{-1} contains the functional groups =C-H (alkenes). They all have twofold boundedness and arise in the low energy and frequency region of the spectrum as bending type vibrations. They are unsaturated and ascribed to functional groups of olefinic (alkenes). They might be found in the biodiesel's unsaturated bond fatty acid methyl esters, like methyl oleate and methyl linoleate [33, 34]. The distinctive peaks, which are located between 1159.2 and 1237.5 cm^{-1}, show that the C-O and C-O-C stretching vibrations are present. In the spectrum, they can also represent the bending vibration of O-CH_3[35, 36]. The peaks at 2855.1-2922.2 cm^{-1}, respectively, show the symmetric and asymmetric stretching vibrations of the C-H alkane groups, which are assigned to the band area of 1379.1 cm^{-1}. These groups, which may be methyl (CH_3) or methylene groups, require a large amount of energy to cause stretching vibrations within their bond, in contrast to the typical C-H bending vibrations of alkene groups found at low energy and frequency region [33, 34] and the bending vibration of C-H methyl groups, while the band at 1744.4 cm^{-1} is ascribed to C=C bending vibrations [37]. There is an aromatic mixture present in the range of 1861–2003 cm^{-1}. It is shown that there is an O-H group extended in carboxylic acid in region 2179.68-2281cm^{-1}. The stretching vibration of =C-H alkene groups is responsible for the peak at 3160.41 cm^{-1}. In the spectrum, they are found at wavenumber 3008 cm^{-1} as opposed to matching alkane C-H stretching groups that are found below 3008 cm^{-1}. The stretching mode of vibration at the peak at 3008 cm^{-1} is attributed to the presence of O-H groups. They are located in the high energy area of the spectrum and are single bounded [11].

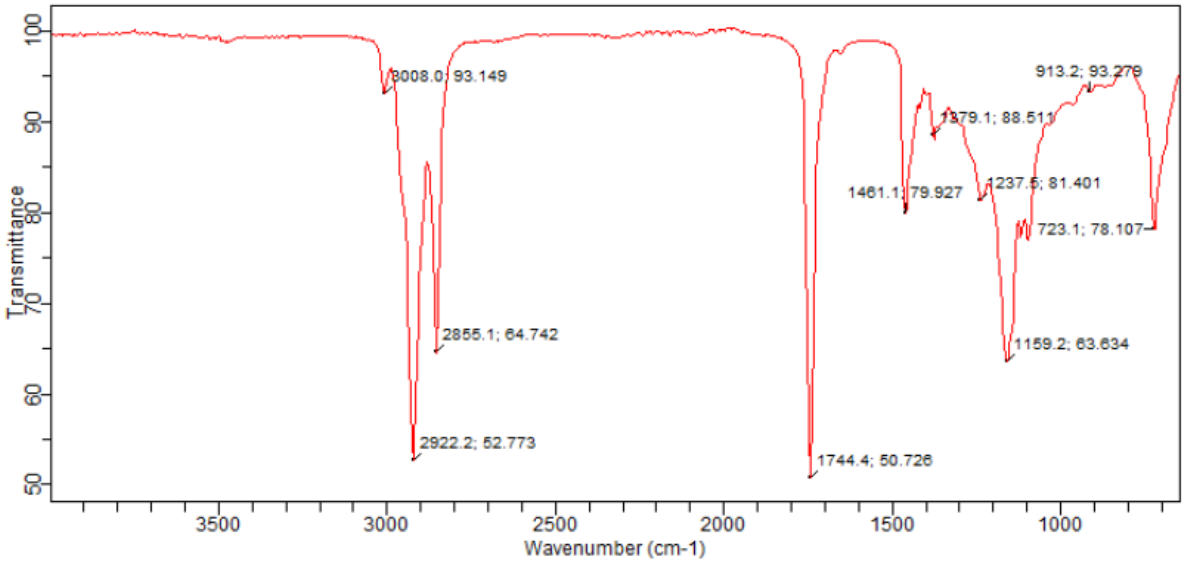

Figure 2: FTIR of water melon seed oil

3.2 Catalyst characterization

The physical features of the periwinkle (P), marble (M) and composite (P+M+Ba) catalysts measured using Brunauer-Emmett-Teller (BET) surface area analyser (Autosorb AS-1 MP, USA)and depicted in Table 4. The table showed that the addition of barium (Ba) with a higher surface area to the composite catalyst resulted in an improvement in its characteristics. After mixing and doping, the composite's pore size grew. This could be explained by the change causing pores to open. There are also presences of more pores as the pore volume increased after doping and blending. This indicates that the doping displaced some unwanted/inert elements from the catalyst.

Table 4: Physiochemical properties synthesized composite catalysts (BET)

Parameters	Periwinkle (P)	Marble (M)	Composite catalyst (P+M+Ba)
Surface area (m^2/g)	282.0	356.0	418.3
Pore size (nm)	2.80	3.00	6.54
Total pore volume (cm^3/g)	0.178	0.186	0.216

The chemical compositions of composite catalyst and its precursors (periwinkle and marble) are presented in Table 5. The major constituents of the catalyst are O, Al, Si, Ca, Fe, and Ba. They contain some transition metals in a little quantity and other alkali and earth alkali metals which are components of heterogeneous catalysts [38, 39]. The high amount of oxygen signifies that the metals were present in their oxides. It could be observed that the precursors contained their characteristic metals; periwinkle has more Ca while marble has more Si. The composite catalyst exhibited the characteristic metals of the precursors, identifying it as Brønsted and Lewis acids. These acids' acidity and catalytic properties are primarily determined by the electro negativity of the interchangeable cations' interlamellar spacing, which are attached to the negatively charged alumina silicate sheets. The doping of Ba with the composite catalyst of periwinkle and marble is evident in

the catalyst. Individually, periwinkle has no Ba but marble has little quantity of Ba. Meanwhile, the composite catalyst contains large quantity of Ba (30.587 wt %). This will help to enhance the catalytic property and prevent side reactions.

Table 5: X-ray fluorescence (XRF) of the composite catalyst and its precursors

	Concentration (wt %)		
Elements	Periwinkle (P)	Marble (M)	Composite catalyst (P + M+ Ba)
O	29.887	44.781	29.572
Na	0.000	0.000	0.000
Mg	1.120	0.000	0.000
Al	1.963	6.189	2.399
Si	1.090	27.744	5.476
P	0.000	0.032	0.000
S	0.217	0.343	4.490
Cl	0.605	0.719	0.485
K	0.103	6.155	0.915
Ca	62.934	5.396	21.850
Ti	0.038	0.756	1.057
V	0.003	0.036	0.203
Cr	0.013	0.028	0.000
Mn	0.099	0.126	0.064
Fe	0.931	6.815	2.360
Co	0.017	0.053	0.006
Ni	0.007	0.002	0.000
Cu	0.055	0.049	0.043
Zn	0.013	0.018	0.012
Sr	0.420	0.146	0.410
Zr	0.000	0.056	0.021
Nb	0.009	0.011	0.005
Mo	0.009	0.004	0.005
Ag	0.006	0.032	0.019
Sn	0.411	0.181	0.000
Ba	0.000	0.216	30.587
Ta	0.026	0.113	0.013
W	0.023	0.000	0.008

Fourier transform infra-red (FTIR) spectroscope of the periwinkle, marble and composite catalysts were performed to identify the organic groups in them and presented in Table 6. Functional groups such as Si-O-Si, weak alkyne stretch, C-H stretch of aromatic bent, C-H stretch of vinyl, and organic silicone are frequently observed in catalysts. These include the Si-O-C, Si-O, double bond C=C, -OH stretch of the primary alcohol, Al–OH–Al, Al–OH–Mg, and Al–OH–O–Si vibrations, as shown in the table and images. Comparing the precursors and composite catalyst, it could be observed that there is presence of bands 998.9 and 980.6 cm-1in periwinkle and the composite catalyst only suggesting that the structural changes attributed to the doping. According to Zatta et al. [40], the FTIR bands at 998.9 and 980.3, are attributed to Ba-O-Ba stretch confirming the presence of Ba in marble and the composite catalyst. The in-plane stretching of Si–O (1080-1447 cm^{-1}) and the Si–O–Si bending (678.4 cm^{-1}) is correlated with an amount of free silica.

Table 6: FTIR analysis of the precursors and composite catalyst

S/N	Group Frequency (cm^{-1}) of catalyst Periwinkle	Marble	Composite	Functional group/Assignment
1	678.4	-	678.4	Si-O-Si deformation
2	711.9-730.6	711.9-730.6	711.9-730.6	Strong aromatic C-H bend,
3	-	771.6	-	Strong aliphatic =C-H and strong aromatic C-H bend, metallic oxide.
4	857.3	-	872.3	Strong alkene=C-H bend, Al-OH-Al
5	-	998.9	980.3	Vinyl C-H out-of-plane bend, Al-OH-Mg, Ba-O-Ba.
6	1080.9-1446.2	-	1095.8-1401.5	Organic siloxane/silicone (Si-O-C), Si-O
7	1640-1994.1	1871.1-1982.9	1796.6-1990.4	Conjugated ketone; strong double bond –C = C-
8	2102.2	2079.9	2109.7	Weak Alkyne $-C \equiv C -$ stretch
9	3652.8	3570.8-3656	3369.5-3637.9	primary alcohol moderately strong free –OH stretch
10	3693.8	3693.8	3809.3	primary alcohol –OH stretch

The morphologies of the periwinkle, marble and composite catalysts are shown in Figures 2a, 2b and 2c respectively. Figure 2a shows that periwinkle has coarse nature with more pores sizes while the marble has small pores sizes spread around its surface (Figure 2b). The coarse nature of periwinkle may be due to higher content of some metallic constituents. The blending of periwinkle and marble showed an improvement in the structure of the composite with increase in number of pores and pore size which is evident in Figure 2c. This suggests that it comprises smaller pores and a larger surface area.

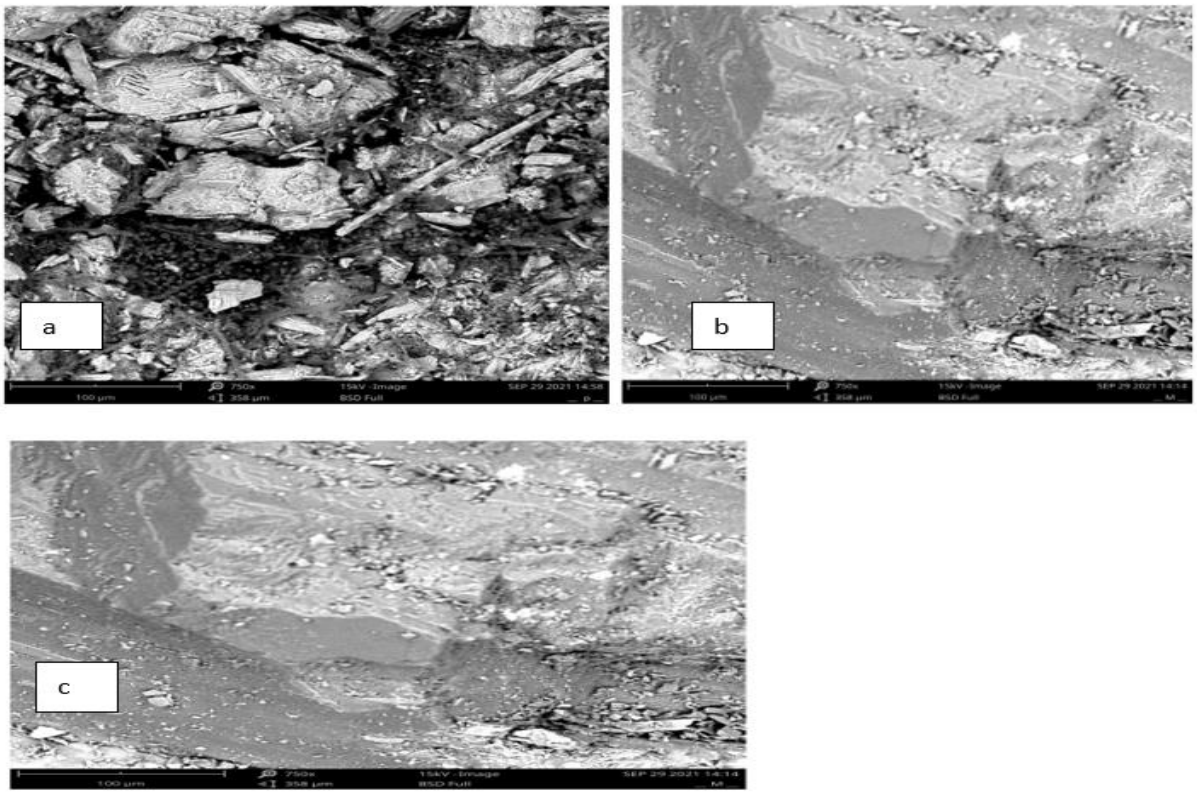

Figure 2: SEM image of (a) periwinkle, (b) marble catalyst and (c) composite catalysts.

Figures 3a, 3b and 3c depict x-ray diffractogram (XRD) of the periwinkle, marble and composite catalyst respectively. The Figure 3a shows that periwinkle belongs to titanium-zirconium while the marble and composite catalysts belong to quartz as shown in Figure 3b. Doping produced graphite, as seen in Figure 3c, which may have been caused by the existence of barium metal. The titanium-zirconium crystals in the periwinkle occurred at between 30 to 40^{o}(Figure 3a) while the quartz and graphite crystals of marble and composite occurred at between 25 to 30^{o} (Figure 3b) and 5 to 10^{o} (Figure 3c) respectively. The presence of titanium zirconium in periwinkle and quartz in marble could be responsible for the Bronsted-Lewis characteristics of the composite catalyst.

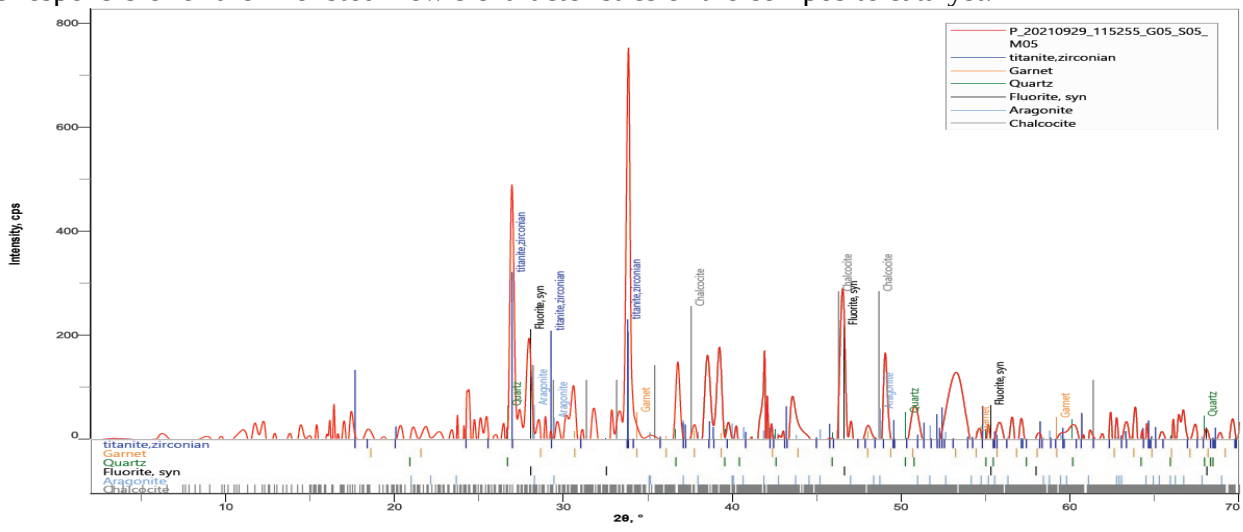

Figure 3a: XRD of periwinkle.

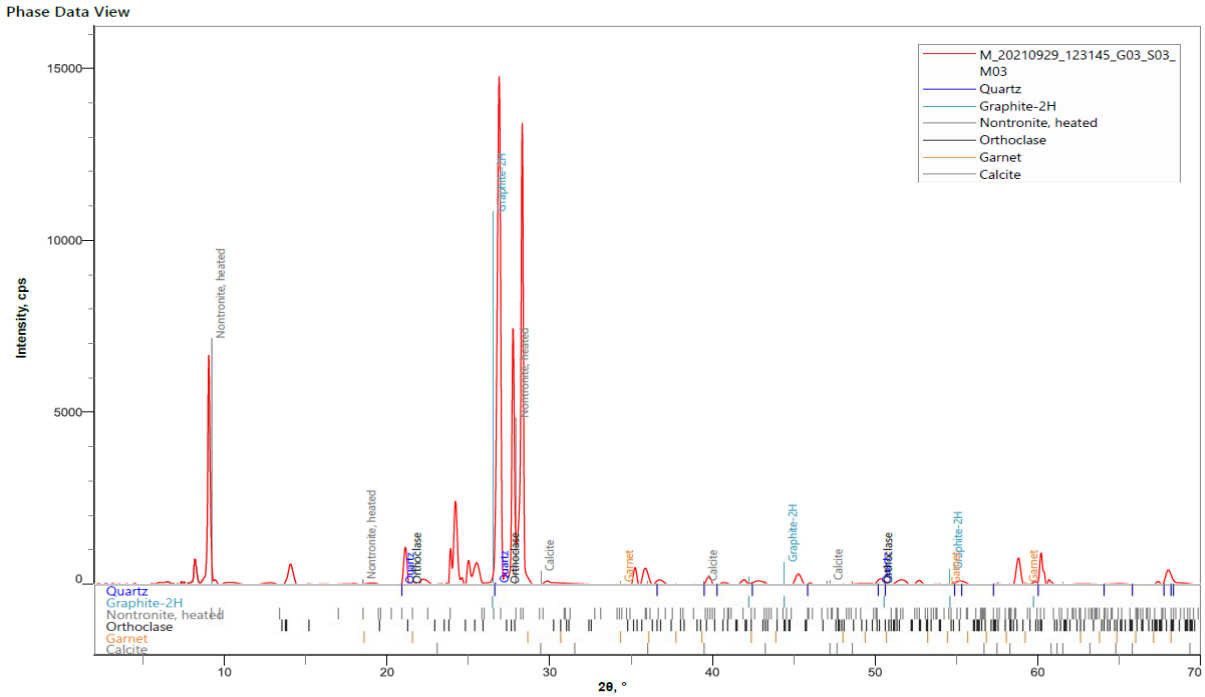

Figure 3b: XRD of the marble

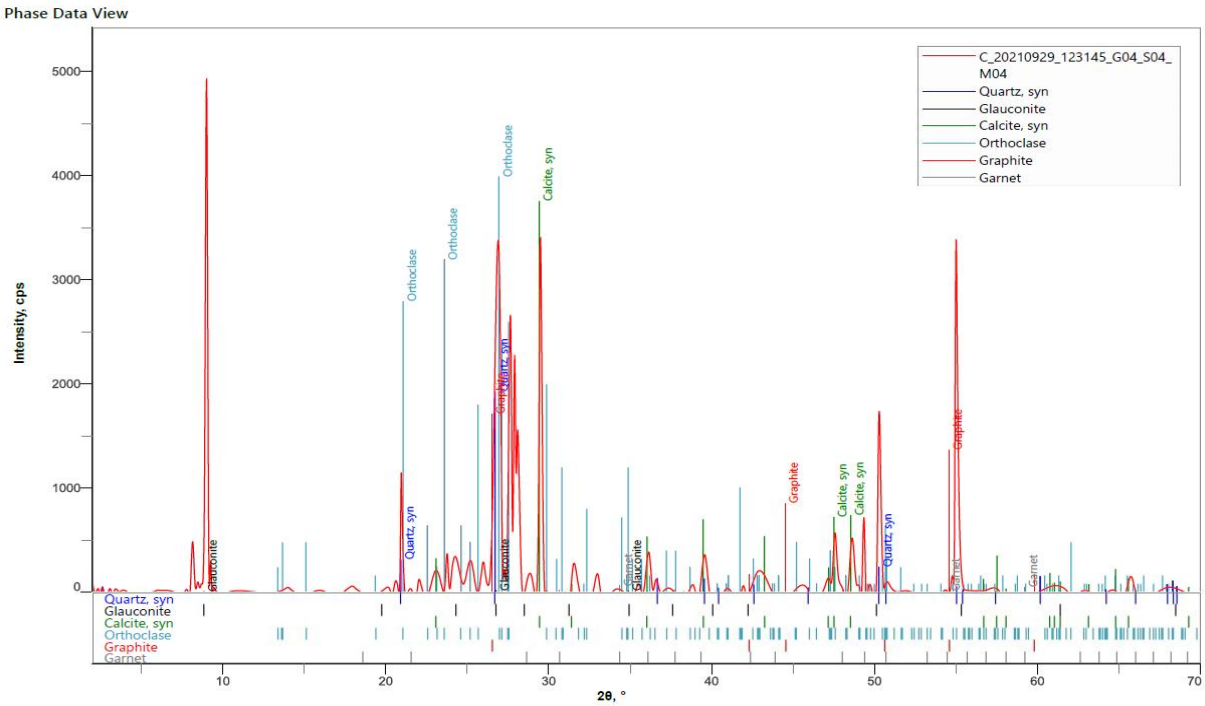

Figure 3c: XRD of composite catalyst.

3.3 Biodiesel yield and characterization

The yield of biodiesel produced was 88.7 wt% and an overview of all the fuel qualities examined and the limitations to which they were compared (ASTM D 6751 standards) may be found in Table 7.In general, biodiesel is denser than petroleum-based fuel. Due to the volumetric determination of the fuel delivered into the combustion chamber, this may have an effect on fuel consumption. At 30 degrees Celsius, the watermelon seed oil biodiesel (WMSOB) density was found to be within the ASTM biodiesel density limitations (Table 7).Additionally, it is noted that the biodiesel's viscosity falls between the ASTM's range of 1.6 to 6.0 Cst. The flash point of a substance is one characteristic that is used to categorize it based on its flammability. Pure methyl ester typically has a flash point of more than 200 °C, which makes them "non-flammable." But not all of the methanol may be eliminated during the biodiesel's manufacture and purification process, leaving the fuel flammable and hazardous to handle and store if the flash point drops below 130^{o}C. It is safe for storage because the flash point was >130^{o}C, which is within the ASTM guideline. High fuel acidity has been associated with deposits in engines and corrosion. The WMSOB has an acid value of 0.6 mg KOH/g. As a result, the biodiesel's acid value is judged to be satisfactory. Oxidation stability is one of the most important factors in deciding the duration that an oil or diesel will last in a particular application. According to Table 4.7, the biodiesel synthesized had an oxidative stability that was within the ASTM-approved values. appropriate given that TAN has an ASTM value of 0.8 mg KOH/g.

The cetane number is a measure of ignition quality. The incomplete combustion of fuels with low cetane levels results in higher emissions. According to ASTM regulations, the cetane index has a lower limit of 47. The WMSOB's cetane number was >50 (using Equation 6), which is higher than the minimum value. This indicates that biodiesel is suitable for use in diesel engines, but the engine's performance will be enhanced if it is blended with a small amount of diesel.

Table 7: WMSOB properties compared with ASTM limits

PROPERTY	UNITS	ASTM METHODS	WMSOB	ASTM LIMITS
Density	kg/m^3	ASTM D-1298	872.8	830-880
Kinematics Viscosity	Cst	ASTM D-445	5.90	1.6-6.0
Flash Point	^{o}C	ASTM D-93	145	≥130
Pour Point	^{o}C	ASTM D-97	5.0	+15 max
Cloud Point	^{o}C	ASTM D-2500	4.0	-15 to 5
Acid Value	mgKOH/g	ASTM D-974	0.60	≤ 0.80
Low Heating Value	MJ/kg		36.4	≥ 35
Aniline Point	(^{o}C)	ASTM D-4737	19.5	
Higher Heating Value	MJ/Kg		70.8	
Oxidative stability	Hour	ASTM D-6751/EN 14112	8	3 min
Cetane number		ASTM D-130	58.02	47 min

3.4 Engine performance and emission characteristics of FAME.

3.4.1 Brake Power, Bp

The net output of the engine is brake power. It is clear from Figure 4 that brake power increases as speed does when the vehicle is fully loaded. This might be explained by a decrease in lubricity at faster speeds. Additionally, the B20 blend engine had the highest brake power, while conventional diesel had the highest brake power at all speeds compared to biodiesel and other blends. This is because biodiesel and its mixes have a reduced calorific value. This is consistent with the findings of Ude et al. [3]. Because there is less biodiesel in B20 than in other blends, the brake power is higher than it is in other mixes.

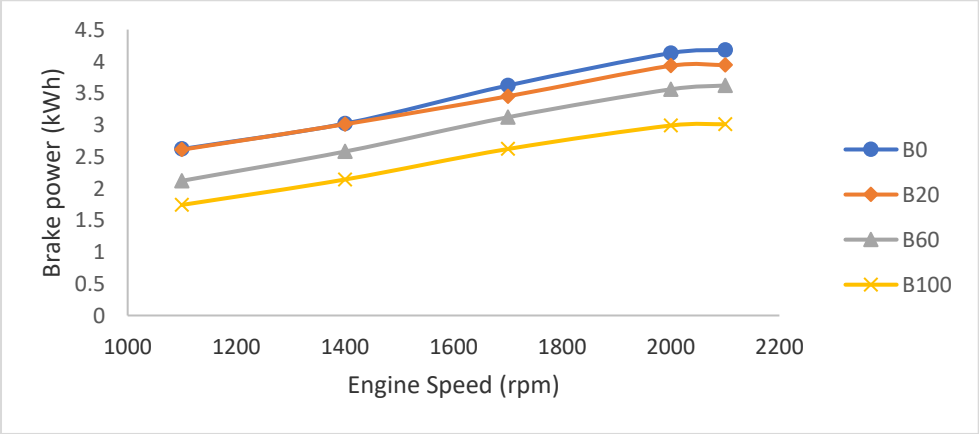

Figure4 : Variation in brake power with engine speed at full load.

3.4.2 Brake thermal efficiency (BTE)

The brake thermal efficiency of the biodiesel engine is shown in Figure 5. According to the figure, the brake thermal efficiency of the engine progressively rises with an increase in engine speed when the engine is fully loaded. It increased to its highest value before declining. This is because at first, as engine speed climbed the torque the engine produced also increased, increasing efficiency. However, at higher rpm (>2000 rpm), more fuel is pumped into the engine cylinder every cycle. As a result of the greater engine speed, this fuel does not have enough time to burn completely, which lowers the engine's efficiency. Furthermore, it was found that some blends and biodiesel have higher thermal efficiency than regular diesel, with B20 blends having the maximum thermal efficiency. This might be explained by their high cetane number, high oxygen content, and low calorific value. The outcome is consistent with what Ude et al. [3] found.

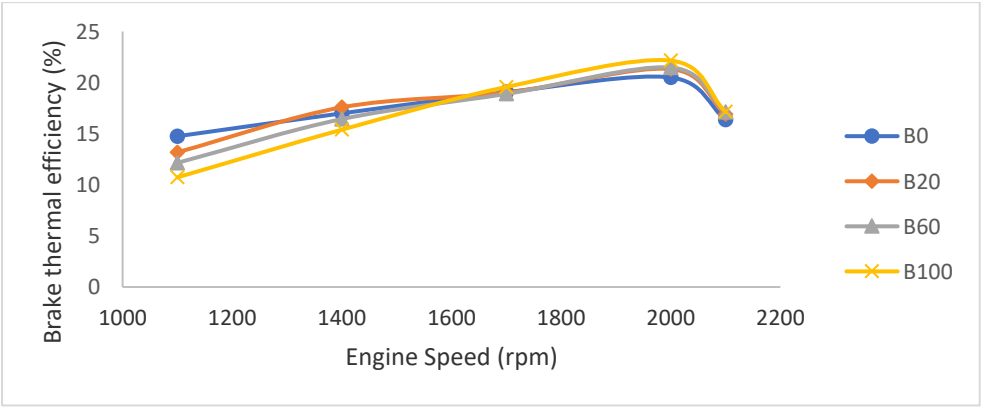

Figure 5: Variation of BTE with engine speed at full load.

3.4.3 Brake specific fuel consumption (BSFC)

The rate of fuel consumption per braking power is known as brake-specific fuel consumption. It is a gauge of how effectively an engine uses the fuel that is given to generate power. Since the engine needs less fuel to accomplish the same amount of work, a lower number of BSFC is preferred. Figure 6 displays the BSFC of watermelon seed oil biodiesel and its mixes. The graph shows that fuel usage rises when biodiesel is used, although this trend will weaken when the quantity of biodiesel in the fuel blend with diesel decreases. The lowest heating value, high density, and high viscosity of B100 may be the causes of its high BSFC. The lowest BSFC is B20. The trend in the data also suggests that the BSFC falls as engine speed rises until the minimum BSFC is reached at roughly 2000 rpm, after which it rises as engine speed rises above 2000. The minimal BSFC was discovered at 2000 rpm and increased till 2200 rpm utilizing FAME from African pear seed oil, according to research by Ude et al. [11], who also noted a similar pattern. Ude et al. [3] achieved a comparable outcome with cottonseed oil FAME at 1300 rpm and a minimal BSFC. The different feedstocks utilized to produce FAME could be the cause of the value discrepancy. When compared to normal diesel, the BSFC of B20 was the lowest and best.

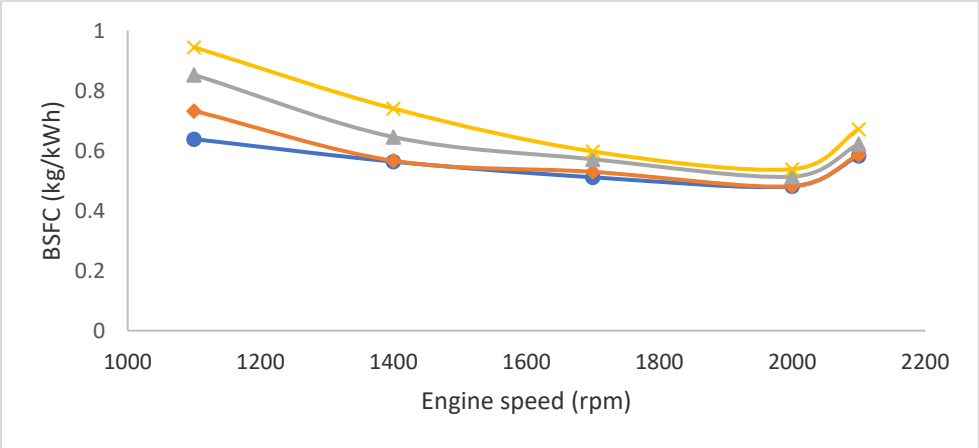

Figure 6: Variation of BSFC with engine speed at full load.

3.4.4 Volumetric efficiency (VE)

The mass of air injected into the engine cylinder divided by the entire mass occupying the displacement volume at intake manifold density is known as volumetric efficiency. The volumetric effectiveness of biodiesel and its blends is shown in Figure 7. According to the data, volumetric efficiency declines as engine speed rises and the proportion of biodiesel in the blend falls. Losses in air flow rate, which happen in throttling circumstances such the air filter, intake manifold, and intake valves, may be to blame for this. Engine speed (also known as induction airspeed) and these losses are inversely correlated.

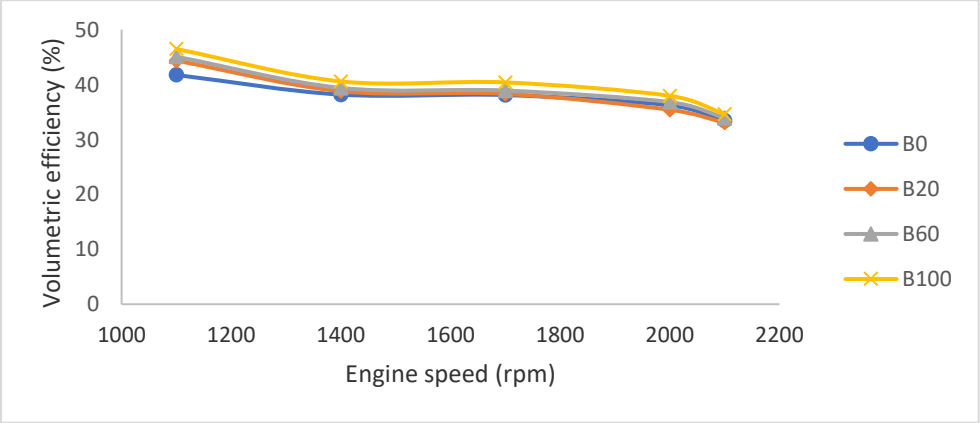

Figure 7: Variation of volumetric efficiency with engine speed at full load

3.4.5 Air/fuel ratio (A/F)

The air/fuel ratio (AFR) of WMSO biodiesel and its mixes is shown in Figure 8. Diesel fuel has a stoichiometric air-to-fuel ratio (AFR) that ranges from 30 to 80, indicating that the mixture in diesel engines is often on the leaner side. This demonstrates that the mixes can operate without modification in a diesel engine. As engine speed increased, the AFR slightly fell. This is because increased friction losses at high speeds also result in increased BSFC. Additionally, when the biodiesel concentration in the fuel mixes rises, the AFR is gradually enhanced. The oxygen content in fuel mixes, which caused complete combustion and increased fuel usage for air, may be to blame for this. The test results showed that for B100 at 2000 rpm, the AFR ratio achieves a maximum value of 90.2:1.

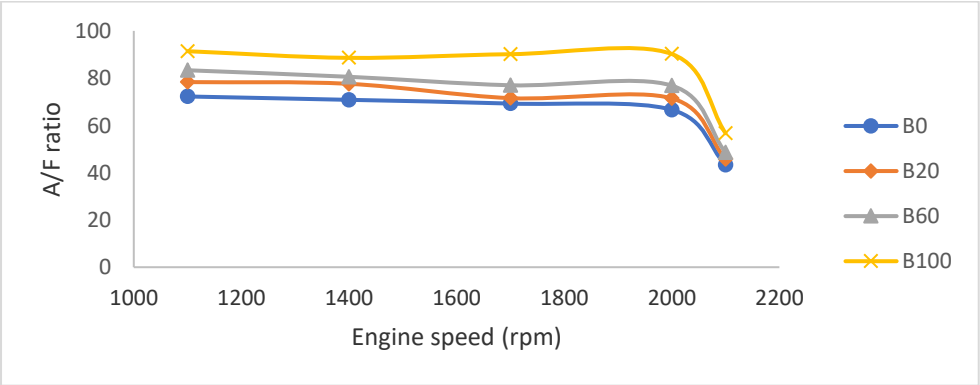

Figure 8: Variation of air/fuel ratio with engine speed at full load.

3.4.6 Emission of CO

The fluctuation in CO emissions of biodiesel with load and mixes in a diesel internal combustion engine is shown in Figure 9. It was found that CO emissions decreased with increasing engine load, which may be related to a drop in the engine's air-fuel ratio. The general declining tendency is influenced by the greater combustion temperature at increasing engine loads. Additionally, the addition of biodiesel results in a reduction in CO emissions. According to Ude et al. [41], it's probable that the oxygen present in the fuel improves full combustion in the cylinder and lowers CO emissions.

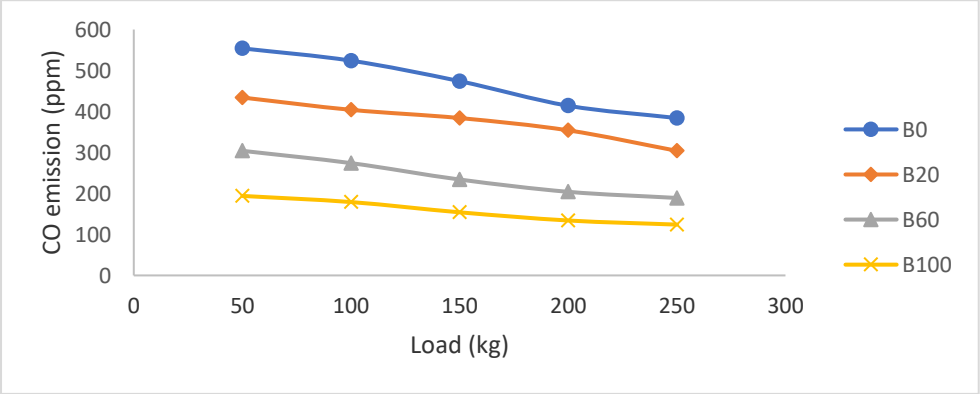

Figure 9: Variation of CO emission with engine speed and load.4.9.2 NOx emission

Figure 10 shows how the biodiesel made from watermelon seeds varies in emissions as a function of load and blend in a diesel internal combustion engine. It was found that emissions rose when engine load and biodiesel concentration both rose. This is mostly caused by a rise in the temperature of the combustion chamber, increased fuel use, and higher oxygen and cetane levels in biodiesel. Ude et al. [41] and Ude et al. [11] found a comparable outcome.

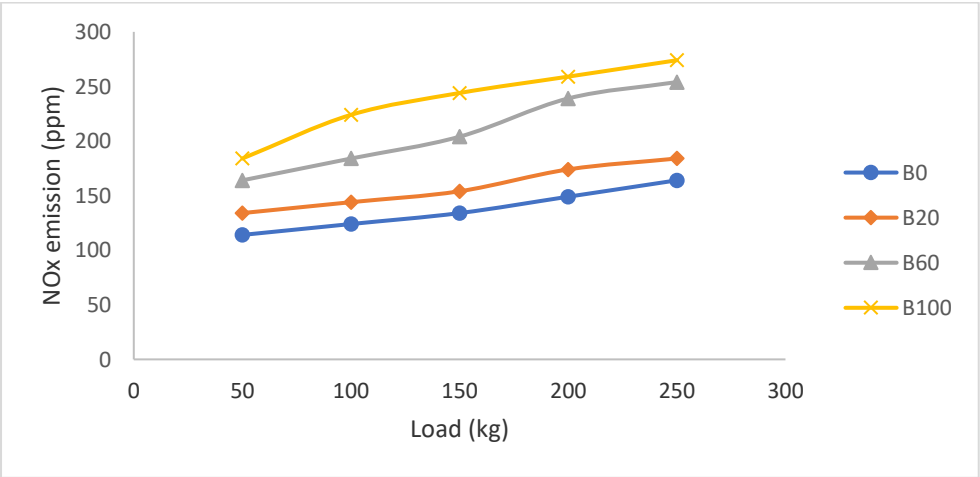

Figure 10: Variation of NOx emission with engine speed and load.

4. Conclusion

This study looked into the efficiency and emission characteristics of diesel engines running on biodiesel made from watermelon seed oil. The oil can be directly transesterified without treatment due to its low acid and fatty acid levels. Watermelon seed oil underwent transesterification to yield 88.7 wt % fatty acid methyl ester (FAME). The yield of methyl ester was greatly impacted by process variables such as reaction time, catalyst concentration, methanol/oil molar ratio, reaction temperature, and agitation speed. The biodiesel produced has standard biodiesel. The engine performance showed that the biodiesel blends had more braking power than regular diesel, while B20 and B0 have comparable thermal efficiencies. Additionally, the blends of biodiesel showed reduced emissions as compared to regular fuel.

Nomenclature

Abbreviation	Meaning
API	American Petroleum
AV	Acid value
BET	Brunauer-Emmett-Teller
B20	Blend with 20% biodiesel
B40	Blend with 40% biodiesel
B100	Blend with 100% biodiesel
BSFC	Brake specific fuel consumption
BTE	Brake thermal efficiency
CP	Cloud point
CR	Compression ratio
DoE	Diameter of Exhaust
FFA	Free fatty acid
FP	Flash point
FTIR	Fourier Transform Infrared
GC-MS	Gas Chromatography Mass Spectrometry
HC	Hydrocarbon
IV	Iodine value
KV	Kinematics viscosity
LEP	Length of Exhaust Pipe
MC	Moisture content
MW	Molecular weight
NCH	Number of cylinder head
PP	Pour point
RI	Refractive index
SEM	Scanning electron microscopy
SV	Swept volume
Sp. gr	Specific gravity
WMSO	Watermelon seed oil
WMSOB	Watermelon seed oil biodiesel

References

[1] Breeze, P. (2018). Diesel Engine. In Piston Engine-Based Power Plants. Diesel Engine System Design
[2] Elendu, C. C., Zhicong. W., Yun, Y., Ude, C. N., Pei-Gao, D., Krzysztof, K. (2023). Yield optimization and fuel properties evaluation of the biodiesel derived from avocado pear waste. Industrial Crops and Products, 191,https://doi.org/10.1016/j.indcrop.2022.115884
[3] Ude, C., N. Onukwuli, O., D. Nwobi, O., C. Anisiji, O., E. Atuanya, C., U. &Menkiti, M., C. (2020a). Performance evaluation of cottonseed oil methyl esters produced using CaO and prediction with an artificial neural network. Biofuels. 11(1), 77–84.
[4] Onukwuli, O. D., Ezeugo, J., Ude, C. N., Nwosu-Obieogu, K. (2022). Improving heterogeneous catalysis for biodiesel production process. Cleaner Chemical Engineering, 3, 100038.
[5] Gashaw, A., &Lakachew, A. (2014). Production of biodiesel from non-edible oil and its properties. International Journal of Science, Environment ISSN 2278-3687 (O) and Technology. 3, 1544 – 1562.
[6] Khan, M., B. Kazim, A., H. & Rab, H., A. (2014). Performance and emission analysis of high purity biodiesel blends in diesel engine. Advances in Mechanical Engineering. https://doi.org/10.1177/1687814020974156.
[7] Odisu, T., Akemu, A., Obahiagbon, K., O. &Anih, E., C. (2019). Comparative studies on the production of biodiesel from shea nut oil by acid catalyzed and supercritical transesterification processes. Journal of Applied Science and Environment Management, 23 (2), 349-357.

[8] Shemelis, N., G. & Marchetti, J., M. (2017). Biodiesel production technologies: Review. AIMS Energy, 5 (3), 425-457.
[9] Aderemi, B. O. & Hameed, B. H. (2010). Production of biodiesel from palm oil. Nigeria Society of Chemical Engineers Proceedings, 40, 135–143.
[10] Azeem, A., A. B. Ayesha, M., & Muhammad, N., S. (2019). Production of biodiesel by enzymatic transesterification of non-edible Salvadora persica (Pilu) oil and crude coconut oil in a solvent-free system. Bioresoures and Bioprocessing, 6 (41), 6217
[11] Ude, C., N. Onukwuli, O., D. Uchegbu, N., N. Umeuzuegbu, J., C & Amulu, N., F. (2021). Evaluation of engine performance and emission of African pear seed oil (APO) biodiesel and its prediction via multi-input-multi-output artificial neural network (ANN) and sensitivity analysis. DOI: 10.1002/bbb.2200; Biofuels, Bioprod. Bioref.
[12] Onoh, I., M.Mbah, G., &Elendu, C., C. (2018). Evaluation of performance of biodiesel produced from african pear (*dacryodesedulis*) seed oil. Explorematics Journal of Engineering and Technology. 2636 – 590.
[13] Dandajeh, H., A. Sanusi, Y., S. &Almadu, T., O. (2020). Exhaust emission characteristics of a gardener compression ignition engine fuelled with rapeseed methyl ester and fossil diesel. Nigerian Journal of Technology, 39 (3), 752-760.
[14] Mofijur, M., Atabani, A., E. Masjuki, H., H. Kalam, M., A. & Masum, B., M. (2013). A study on the effects of promising edible and non-edible biodiesel feedstocks on engine performance and emissions production: A comparative evaluation. Renewable and Sustainable Energy Reviews, Elsevier, 23, 391-404.
[15] Akhtar, M., T. Ahmad, M., Ramadan, M., F. Makhkamov, T., Yuldashev, T., Mamarakhimov, O., Munir, M., Asma, M., Zafar, M., & Majeed, S. (2023). Sustainable production of biodiesel from novel non-edible oil seeds (*Descurainia Sophia L.*) via green nano CeO_2 catalyst. Energies, 16 (3), 1534. https://doi.org/10.3390/en16031534.
[16] Aransiola, E., F. Ojumu, T., V. Oyekola, O., O. &Ikhuomoregbe, D., I. O. (2012). A study of biodiesel production from non-edible oil seeds: a comparative study. The Open Conference Proceedings Journal, 3, 18-22.
[17] Adaileh, W. M. &AlQdah, K. S. (2018). Performance of diesel engine fuelled by a biodiesel extractedfrom a waste cocking oil,Energy Pocedia, 18, 1317 – 1334.
[18] Bjorn, S; S. and Capareda, S. (2015). A comperative study on the engine performance and exhaust emissions of biodiesel from various vegetable oils and animal fat.Journal of Sustainable Bioenergy Systems 05 (03) 89-103.
[19] Som, S., Longman, D. E. Ramirez, A. I. & Aggarwal, S. K. (2010). A comparison of injector flow and spray characteristics of biodiesel with petrodiesel. Fuel, 89, 4014-4024.
[20] Pereira, F., M. Velasquez, J., A. Riechi, J., L. Teixeira, J., Ronconi, L., Riolfi Jr, S., Karas, E., L. Abreu, R., &Travain, J., C. (2020). Impact of pure biodiesel fuel on the service life engine-lubricant: A case study. Fuel 261, 116418; https://doi.org/10.1016/j.fuel.116418.
[21] Gulzar, M., Masjuki, H., H. Varman, M., & Kalam. (2016). Effects of biodiesel blends on lubricating oil degradation and piston assembly energy losses. Proceedings of the ICE-Energy. 111, 713-721.
[22] Fashe Li, Zihao Ni, Zihao and Hua, W. (2019). Effect of biodiesel components on its lubrication performance. The journal of Materials Research and Technology. 8 (5) DOI: 10.1016/j.jmrt.06.011.
[23] Fazal, M., A. Haseeb, A. S. M., A. &Masjuki, H., H. (2013). Investigation of friction and wear characteristics of palm biodiesel. Energy Conversion and Management, 67, 251-256.
[24] Fathurrahman, N., A. Auzani, A., S. Zaelani, R., Anggarani, R., Aisyah, L., Maymuchar. &Wibowo, C., S. (2023). Lubricity properties of palm oil biodiesel blends with petroleum diesel and hydrogenated vegetable oil. Journals / Lubricants, 11 (4), 176. https://doi.org/10.3390/lubricants 11040176
[25] Esonye, C., Onukwuli, O.D., Ofoefule, A.U., Ogah, E.O., 2019. Multi-input multi-output (MIMO) ANN and Nelder-Mead's simplex-based modelling of engine performance and combustion emission characteristics of biodiesel-diesel blend in CI diesel engine. Appl. Therm. Eng. 151, 100–114. https://doi.org/10.1016/j. applthermaleng.2019.01.101.
[26] Shaah, M. A., H. Hossain, Md. & M. Allafi, F. A., S. Ismail, A. A., N. Ab Kadir, M., O. & Ahmad, M., I. (2021). A review on non-edible oil as a potential feedstock for biodiesel: physicochemical properties and production technologies. National Library of Medicine, 11 (40), 25018-25037.
[27] Christopher, L., H. Donald, J., & Don E. (2010). Effects of diesel and biodiesel blends on engine performance and efficiency, 11, 20-26.
[28] Aboje, A. A., Ohile, S. O., Uthman, H., Olutoye, M. O., Nwachukwu, C. A. (2023). Optimization and characterization of biodiesel production from Desert Date seed oil (Balanites aegyptiaca) via transesterification reaction. Journal of Energy Technology and Environment, 5(2), 181-186.
[29] American Society for Testing and Materials ASTM D6751 (1973), Standard Specification for Natural (Vegetable Oil) and biodiesel, ASTM International, West Conshohocken, PA, 1973, www.astm.org.

[30] American Society for Testing and Materials. Standard test method for determination of iodine number of activated carbon. Philadelphia, PA: ASTM Committee on Standards (1986).
[31] Manuit J, Statit P (2007) Biodiesel synthesis from transesterificationby clay-based catalyst. Chiang Mai J Sci 34(2):201–207.
[32] Ogunsuyi, H. O. (2015). Production of biodiesel using african pear (*Dacryodes edulis*) seed-oli as feedstock. Academia Journal of Biotechnology, 3 (5), 085-092.
[33] Saifuddi, N. Refal, H. & Kumaran, P. (2017). Performance and emission characteristics of micro-gas turbine engine fuelled with bioethanol-diesel-biodiesel blends. Institute of Sustainable Energy (The National Energy University), 0326 - 4030.
[34] Jimoh, O. S. Adesoye, P. Adeyemi, A. A. &Ikyaagba, E. T. (2012). Forest structure analysis in the Oban division of Cross River National Park, Nigeria. Journal of Agricultural Science and Technology, 2, 510-518.
[35] John, C. (2000). Interpretation of infrared spectra, a practical approach. Encyclopedia of Analytical chemistry, 10815–10837.
[36] Isah, Y., Yousif, A. A., Feroz, K. K., Suzana, Y., Ibraheem, A. & Soh, A. C. (2015).Comprehensive characterization of napier grass as feedstock for thermochemical conversion. Energies Journal, 8, 3403-3417.
[37] Shuit, S. H. Lee, K. T. Kamaruddin, A. H. & Suzana, Y. (2010). Reactive extraction and situesterification of Jatropha Curcas L. seeds for the Production of Biodiesel. Fuel, 89 (2), 527-530.
[38] Sani, Y. M., Daud, W. M. A. W. &AbdulAziz, A. R. (2012). Biodiesel feedstock and production technologies: successes, challenges and prospects. Chapter Metrics Overview. DOI: 10.5772/52790.
[39] Ude, C. N. &Onukwuli, O. D. (2019). Kinetic modeling of transesterification of gmelina seed oil catalyzed by alkaline activated clay (NaOH/clay) catalyst. Reaction Kinetics, Mechanism and Catalysis, 127, 1039-1058.
[40] Zatta, L., Ramos, L. P., Wypych, F. (2013). Acid-activated montmorillonites as heterogeneous catalysts for the esterification of lauric acid with methanol. Appl Clay Sci 80–81:236–244.
[41] Ude, C. N., Onukwuli, O. D., Umeuzuegbu, J. C., Chukwuka, C. C. (2020b). Heterogeneously catalyzed methanolysis of gmelina seed oil to biodiesel. Chemical Engineering and Technology, 10.1002/ceat.202000080.